J Mater Sci (2008) 43:1745–1748
DOI 10.1007/s10853-007-2399-7

LETTER

Viscoelasticity and macromolecular topology in single-site catalyzed polyethylene

**Juan F. Vega · Dorian Polo-Cerón ·
Santiago Gómez-Ruíz · Sanjiv Prashar ·
Mariano Fajardo · Javier Martínez-Salazar**

Received: 20 September 2007 / Accepted: 11 December 2007 / Published online: 27 December 2007

Introduction

The relationship between polymer chain topology, i.e. long chain branching (LCB), and rheological properties in polyolefins obtained using single-site catalysts has been the topic of major scientific activity since the late 1990s [1–14]. Indeed, melt-state rheological measurements are being considered as one of the most sensitive methods for detecting sparse LCB in polyethylene (PE) [1, 15]. For example the flow activation energy, E_a, related to the temperature dependence of viscoelastic properties, is altered by the presence of LCB, and the cross-point frequency between storage and loss moduli, ω_x, and the cross-point modulus, G_x, are also very sensitive features to the molecular architecture [16–18]. In this context, the study of these properties can give us information about the relationship between polymer chain topology and catalyst structure. In this work, a set of PE samples was synthesized using different metallocene catalysts. The main objective is to find relationships between chemical structure of the catalysts and polymer chain architecture by rheological testing. This is an interesting task as there is still a lack of information in the literature concerning how the catalyst structure affects the creation of LCB during polymerization [15]. The PE samples were synthesized using the catalysts shown in Table 1, together with MAO as co-catalyst. The synthesis of the samples was carried out under the same experimental conditions: a reactor temperature of 20 °C, an ethylene pressure of 2 bar, 3×10^{-5} mol L^{-1} of metallocene concentration, and a molar ratio MAO (methyl aluminoxane)/metallocene of 3,000 [17–21]. The metallocene catalysts were prepared using synthetic protocols that we have previously reported [20, 21]. The molecular properties of the polymer samples obtained by size exclusion chromatography analysis are listed in Table 1. The details about the experimental procedures are described elsewhere [18, 19]. It has been very difficult to estimate the molecular features in the case of C4 sample, probably due to extremely high molecular weight. In this case we have estimated molecular weight and polydispersity index by rheological methods.

The materials were stabilized with 1.0 wt.% Irganox 1010 to avoid degradation at high temperatures. The rheological measurements were carried out using parallel plate geometry (15 mm diameter). Frequency sweeps in the linear viscoelastic regime were performed with a Bohlin CVO rheometer in the angular frequency range between 0.006 and 60 rad s^{-1}. The linear viscoelastic regime has been located by previous strain sweeps. The measurements have been performed in the temperature range between 145 and 190 °C and the time-temperature superposition principle (TTSP) applied to a reference temperature of $T_0 = 190$ °C. From these results, the characteristic features described above (E_a, ω_x, and G_x) have been obtained for the materials under study (see Table 1).

The material labeled as A0 has been synthesized by using the $[Zr(\eta^5\text{-}C_5H_5)_2Cl_2]$ catalyst (A), which is the simplest structural fragment used in this study. This catalyst has been previously reported to produce LCB [2, 14]. The sample shows a very high E_a value and a significant elastic character, in spite of the very narrow molecular

J. F. Vega (✉) · J. Martínez-Salazar
Departamento de Física Macromolecular, Instituto de Estructura de la Materia, CSIC, Serrano 113 bis, 28006 Madrid, Spain
e-mail: imtv477@iem.cfmac.csic.es

D. Polo-Cerón · S. Gómez-Ruíz · S. Prashar · M. Fajardo
Departamento de Química Inorgánica y Analítica, E.S.C.E.T., Universidad Rey Juan Carlos, 28933 Móstoles (Madrid), Spain

Table 1 Molecular and rheological properties of the materials studied

Catalyst	Sample	M_w (kg mol^{-1})	M_w/M_n	E_a (kJ mol^{-1})	ω_x (rad s^{-1})	G_x (kPa)
$[Zr(\eta^5\text{-}C_5H_5)_2Cl_2]$	A0[a]	170	2.3	97.9	7.1×10^{-1}	15.0
$[Zr(\eta^5\text{-}C_5H_5)(\eta^5\text{-}C_5H_4\{CHMeC_{14}H_9\})Cl_2]$	B1	384	4.4	–	3.1×10^{-3}[b]	< 20.0
$[Zr(\eta^5\text{-}C_5H_4\{CHMeC_{14}H_9\})_2Cl_2]$	B2	720	4.0	–	5.1×10^{-5}[b]	< 20.0
$[Zr(\eta^5\text{-}C_5H_5)(\eta^5\text{-}C_5H_4\{CHMePh\})Cl_2]$	C1	480	8.8	22.9	1.1	105
$[Zr(\eta^5\text{-}C_5H_5)(\eta^5\text{-}C_5H_4\{CHBu^tPh\})Cl_2]$	C2	600	5.0	25.8	3.3×10^{-1}	115
$[Zr(\eta^5\text{-}C_5H_4\{CHMePh\})_2Cl_2]$	C3	1,055	4.8	25.0	5.0×10^{-2}	125
$[Zr(\eta^5\text{-}C_5H_5)(\eta^5\text{-}C_5H_4\{CHPr^iPh\})Cl_2]$	C4	n.d. [4,500]	n.d. [5.0]	26.2	9.0×10^{-4}[b]	<120
$[Zr\{Me_2Si(\eta^5\text{-}C_5Me_4)(\eta^5\text{-}C_5H_3\{CHMeC_{10}H_7\})_2Cl_2]$	D1	79.3	4.4	53.9	34.7	90.5
$[Zr\{Me_2Si(\eta^5\text{-}C_5Me_4)(\eta^5\text{-}C_5H_3\{CHMePh\})_2Cl_2]$	D2	197	7.1	55.0	1.1	85.3

[a] Synthesized with $[Zr(\eta^5\text{-}C_5H_5)_2Cl_2]$, a known catalyst able to produce LCB [1, 15]

[b] Estimated values by horizontal shifting to a master curve (see text)

The values between brackets have been estimated from the rheological properties

weight distribution ($M_w/M_n = 2.3$). This is revealed by the low value of G_x, which is one order of magnitude lower than in the rest of the samples (see Table 1). These are characteristic features of polyolefins with high LCB content like low-density PE [17]. This material can be clearly distinguished from those obtained by means of catalyst C series. All the samples show the characteristic E_a value of high-density PE (around 25 kJ mol^{-1}) [18]. The linear viscoelastic response of these materials (storage modulus, G'; and loss modulus, G'') referred to the average relaxation time of the samples, τ_x, as given by the reciprocal cross-point frequency, $1/\omega_x$ (see Table 1), can be observed in Fig. 1. These samples show the typical viscoelastic fingerprint of linear PE with very high molecular mass. The relaxation times follow the expected trend of reptation motion with the molecular mass of linear polyethylene ($\tau_x \sim M_w^{3.4}$) [22].

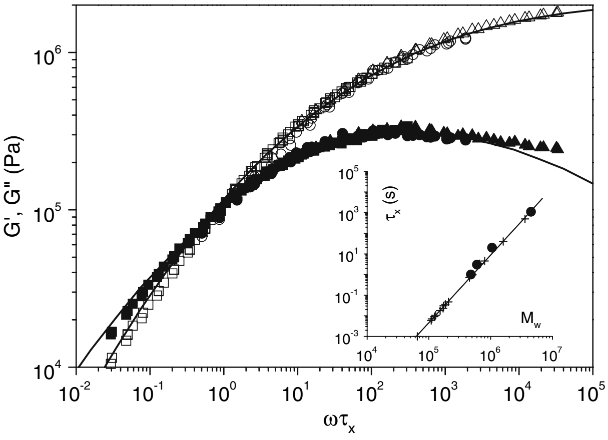

Fig. 1 Linear viscoelastic moduli versus normalized angular frequency, $\omega\tau_x$, of linear C series. Storage modulus, G' (open symbols), and loss modulus, G'' (close symbols), for (□■) C1, (○●) C2, and (△▲) C4. The inset shows the plot of the relaxation time versus molecular mass for (●) linear PE series and (+) results from the literature [21, 22]

It is important to note that the catalyst C series is characterized by the phenyl substituents in the cyclopentadienyl (Cp) ring of the basic fragment (catalyst A). These results agree with those found by Kokko et al. [6] and Piel et al. [16]. In both studies the samples obtained from catalyst A with alkyl (methyl and butyl)-substituted Cp rings possessed a linear structure. Piel et al. suggested that a substituted Cp configuration determines LCB formation, and therefore the open aperture gap in catalyst A should be the cause for the formation of LCB structures.

Notwithstanding, the inclusion of extremely bulky substituents based on anthracene in the Cp ring leads to materials with a particular linear viscoelastic response. Both samples obtained with catalyst series B are characterized by an extremely high elastic character, as G' is higher than G'' in the whole range of frequencies available. The cross-point modulus is not obtained experimentally, but it can be envisaged that G_x is lower than 20 kPa (as in the case of branched sample A0). This is a typical feature of polymers with LCB and very high molecular mass. A master curve has also been constructed to compare the results of the branched (A and B) and the linear samples (C). The result is plotted in Fig. 2. The branched series show a very interesting behavior when the linear response is reduced to the same relaxation time as the linear series. A characteristic dilution of G' and G'' together with a broader relaxation time spectrum of the branched polymers are clearly seen in Fig. 2, accounting for the strong effect of LCB in molecular dynamics.

However, the materials obtained from D catalyst series display a more remarkable behavior [4–10, 15]. These are *ansa*-metallocene catalyst systems with bulky substituents (1-phenylethyl and 1-(1-naphthyl)ethyl) in the Cp rings. The temperature dependence of the linear viscoelastic

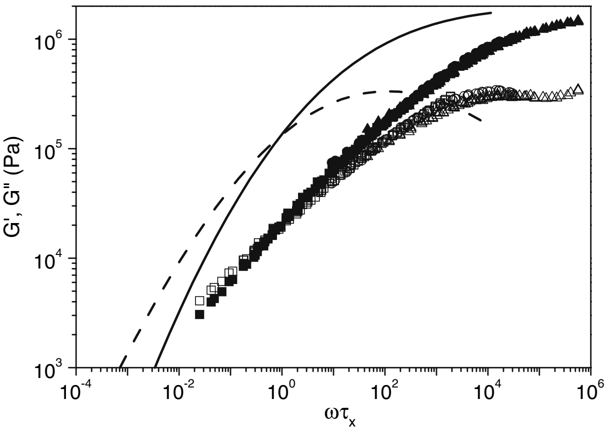

Fig. 2 Linear viscoelastic moduli versus normalized angular frequency, $\omega\tau_x$, of branched PE A and C series. Storage modulus, G' (open symbols), and loss modulus, G'' (close symbols), for (□■) A0, (○●) B1, and (△▲) B2. The lines indicate the result obtained for linear C series: solid line, G', and dashed line, G''

properties is quite particular. As observed in Fig. 3, the TTSP does not apply in the phase angle, δ ($\tan\delta = G''/G'$) for these samples. In fact, the low-frequency properties show more pronounced temperature dependencies than the high-frequency properties. This means the flow activation energy, E_a, is different depending on the frequency (or modulus) domain, in agreement with previous observations made for LCB polyolefins obtained from other *ansa*-metallocene [4–10] and constrained geometry catalysts [11–13]. This complex thermorheological behavior could arise from multiple relaxation mechanisms with different temperature dependencies, resulting from macromolecules with different configurations or molecular topologies. The E_a values listed in Table 1 for this series correspond to the high-frequency domain.

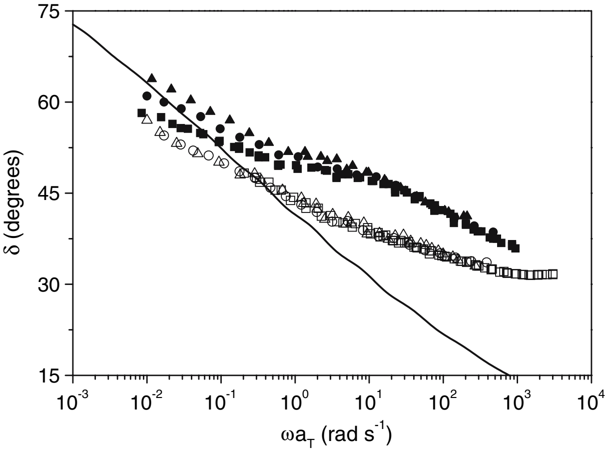

Fig. 3 Phase-angle dependence of angular frequency at a reference temperature of 190 °C for different materials: (solid line) complete linear C series; (open symbols) branched A0, and (close symbols) branched D1. The different symbols correspond to different temperatures between T_m and 190 °C: (□■) 145 °C, (○●) 167.5 °C, and (△▲) 190 °C

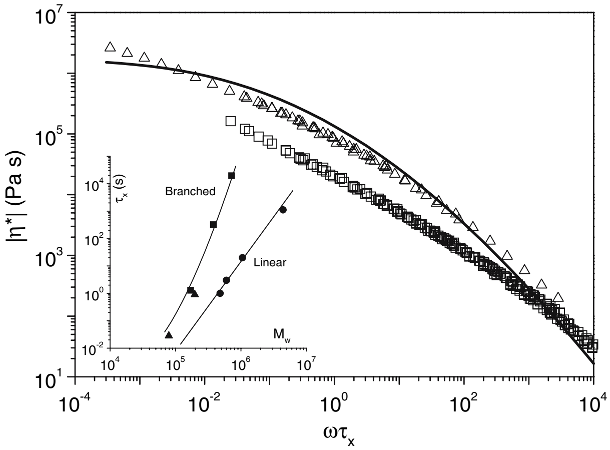

Fig. 4 Normalized to τ_x complex viscosity curves of all the materials studied at 190 °C: (solid line) linear C series, (□) branched A and B series, and (△) branched D series. The inset shows the plot of the relaxation time versus molecular mass for (●) linear C series, (■) branched A and B series, and (▲) branched D series

The complex viscosity, $|\eta^*|$, of all the materials studied has been reduced to the same relaxation time in Fig. 4. Complex and shear viscosity, $\eta(\dot{\gamma})$, are empirically related by the Cox–Merz rule [23], which is generally applicable to homogeneous polymer melts; so some interesting conclusions about the behavior of materials during processing can be anticipated. Considering that the differences in polydispersity index are not so high (see Table 1), the viscosity shape disparity found in Fig. 4 can be ascribed to the diverse molecular topologies as we have discussed above. Once again, it is possible to classify the materials in to three different groups. Linear B series shows a clear transition zone between the limiting zero-shear viscosity and the shear-thinning region at high frequencies (shear rates). Branched series A, B, and D show a prominent pseudoplastic behavior, particularly in the latter case. No sign of a transition exists in these samples, as the zero-shear viscosity "plateau" is shifted to very low frequencies, corresponding to materials with very long relaxation time and broad relaxation time distribution. The trend in D series is to reach higher values of the zero-shear viscosity, as occurs in those systems for which mechanical relaxation in the terminal zone is hindered due to the presence of long branches. No conclusions about zero-shear viscosity can be drawn in the case of A and B series, as no leveling-off of $|\eta^*|$ is observed at low frequencies. However, the viscosity at intermediate-to-high frequencies (shear rates) is around one order of magnitude lower than in the rest of the samples, which points to less resistance to flow and good processing behavior, as in the case of low-density PE. A comparison of the different series has been made in terms of the relaxation time obtained from the reciprocal cross-point frequency, $\tau_x = 1/\omega_x$. The characteristic values of the relaxation time are two orders of magnitude or higher than those corresponding to the linear homologues with the same molecular weight, which is the common sign that reptation is hindered because of the presence of LCB (see the inset in Fig. 4).

The diverse catalysts studied show different abilities for the incorporation of LCB in the macromolecular structure. The polymers synthesized by means of catalysts A (unsubstituted Cp) and B (extremely bulky substituted Cp) show the typical viscoelastic fingerprint of samples with high amounts and/or very long branches. The samples obtained with catalysts C (substituted Cp) show the unique viscoelastic response that corresponds to linear macromolecules with characteristic ultrahigh molecular mass. Finally, the polymers obtained with *ansa*-metallocene catalysts D show a very complex response, representative of materials with macromolecules with different topologies.

Acknowledgements J.F. Vega acknowledges the Ministerio de Educación y Ciencia (MEC), Spain, for a Ramón y Cajal Tenure (2006). We would like to thank the MEC (Projects MAT2006-0400 and CTQ2005-07918-C02-02/BQU), the Comunidad de Madrid (Project S-0505/PPQ-0328), and the Universidad Rey Juan Carlos (graduate fellowship for D. Polo-Cerón) for financial support.

References

1. Vega JF, Santamaría A, Muñoz-Escalona A, Lafuente P (1998) Macromolecules 31:3639
2. Vega JF, Fernández M, Santamaría A, Muñoz-Escalona A, Lafuente P (1999) Macromol Chem Phys 200:2257
3. Aguilar M, Vega JF, Sanz E, Martinez-Salazar J (2001) Polymer 42:9713
4. Malmberg A, Kokko E, Lehmus P, Löfgren B, Seppälä J (1998) Macromolecules 31:8448
5. Malmberg A, Liimatta J, Lehtinen A, Löfgren B (1999) Macromolecules 32:6687
6. Kokko E, Malmberg A, Lehmus P, Löfgren B, Seppälä JV (2000) J Polym Sci: Polym Chem 38:376
7. Kokko E, Pietikäinen P, Koivunen J, Seppälä JV (2001) J Polym Sci: Polym Chem 39:3805
8. Kokko E, Wang W-J, Seppälä JV, Zhu S (2002) J Polym Sci: Polym Chem 40:3292
9. Gabriel C, Kokko E, Löfgren B, Seppälä J, Münstedt H (2002) Polymer 43:6383
10. Malmberg A, Gabriel C, Steffl T, Münstedt H, Löfgren B (2002) Macromolecules 35:1038
11. Wood-Adams PM, Dealy JM (2000) Macromolecules 33:7481
12. Wood-Adams PM, Dealy JM, Degroot AW, Redwine OD (2000) Macromolecules 33:7489
13. Wood-Adams P, Costeux S (2001) Macromolecules 34:6281
14. He C, Costeux S, Wood-Adams P (2004) Polymer 45:3747
15. Piel C, Stadler FJ, Kaschta J, Rulhoff S, Münstedt H, Kaminsky W (2006) Macromol Chem Phys 206:26
16. Utracki LA, Schlund B (1987) Polym Eng Sci 27:367
17. Vega J, Aguilar M, Peón J, Pastor D, Martínez-Salazar J (2002) e-polymers 042:1
18. Vega JF (2003) Recent Res Dev Macromol 7:29
19. Gómez-Ruiz S, Prashar S, Sánchez-Barba LF, Polo-Cerón D, Fajardo M, Antiñolo A, Otero A, Maestro MA, Pastor CJ (2007) J Mol Catal A: Chem 264:260
20. Polo-Cerón D, Gómez-Ruiz S, Prashar S, Fajardo M, Antiñolo A, Otero A, López-Solera I, Reyes ML (2007) J Mol Catal A: Chem 268:264
21. Polo-Cerón D, Gómez-Ruiz S, Prashar S, Fajardo M, Antiñolo A, Otero A (2007) Collect Czech Chem Commun 72:742
22. Vega JF, Aguilar M, Martínez-Salazar J (2003) J Rheol 47:1505
23. Cox WP, Merz EH (1958) J Polymer Sci 28:619